POST-BUCKLING ASSOCIATED INTERLAMINAR DELAMINATION IN A CARBON FIBER REINFORCED PLASTIC (CFRP) LAMINATE

A. K. El-Senussi

Aeronautical Engineering Department,
Al-Fateh University, Tripoli, Libya
E-mail, elsen2005@yahoo.com

الملخص

تتناول هذه الورقة تحليل نظري لمسألة الانفصال الجزئي بين طبقات شريحة ارثوتروبية مقوّاة طوليا وواقعة تحت تأثير انفعال ضغط منتظم في مستوى الشريحة آخذاً في الاعتبار التأثيرات المرنة للأجزاء الطرفية الملتصقة.

انبعاج الجزء المنفصل وما قد يتبعه من اتساع رقعة الانفصال تم تناوله بالتحليل مع تحديد الظروف الحرجة المؤدية إلى كسر الروابط الطبقية البينية وذلك باتباع سلوك الأعمدة المحملة محوريا والكمرات المدعمة بقواعد مرنة. معادلتان تفاضليتان تمثلان الجزء المنفصل والجزئين الطرفيين الملتصقين تم حلهما وربطهما عن طريق شروط الإستمرارية على طول الخط الفاصل بين الانبعاج والجزء الملتصق للشريحة. هذا التحليل مكّن من حساب طاقة المرونة المخزونة في الشريحة المركبة ومعدل التحرير الجزئي لهذه الطاقة اللازم لسريان التصدع البيني الذي وجد أنه لا يحدث إلا في مرحلة مابعد انبعاج الجزء الوسطي المنفصل للشريحة.

ABSTRACT

A theoretical analysis is presented for interlaminar separation of a through width central debond in a typical fiber reinforced plastic orthotropic layer, taking into account the elastic end effects of a matrix rich layer at the delaminating fronts between debonded and undebonded areas.

The post-buckling behavior of the separated portion with consequent possible further delamination is analyzed and the critical conditions leading to interlaminar splitting are determined.

Two differential equations based on beam-column theory are produced for the debonded and attached portions. These equations have been solved and linked together by imposing the continuity conditions along the delamination front marking the boundary between the two parts of the layer. The solution allowed using an energy release rate criterion to obtain the critical strains and determine their interactions at the post-buckling stage. Numerical results in graphical form showed that delamination is not possible unless the debonded part buckles.

KEYWORDS: Interlaminar separation; Post-buckling; Orthotropic layer; Delamination; Energy release rate.

INTRODUCTION

The delamination problem emanating from a pre-existing initial bulge (blister) is analyzed for fibrous laminated plates in [1]. It has been found that delamination may well take place while the in-plane load in the blister layer P_1, is below the Euler buckling load P_E. This may not be the case when the initial debonded layer is perfectly flat when the load is first applied. If a uniform applied strain ε is assumed, delamination will not grow as long as the initially debonded area is flat [2]. However, delamination is possible if the debonded portion buckles. Therefore, the problem can only be assessed through post-buckling analysis. If the extent of delamination and its consequences on the integrity of a certain laminate are the main concern, then, the problem is far more serious than the case analyzed in [1]. In fact, the behaviour is progressive where a pre-loading bulge is present and therefore, can be controlled unlike the initially flat debond case when post-buckling events may be sudden and catastrophic. However, it may happen that delamination will not occur following buckling, in which eventuality, the problem can be treated exactly in the same way as when $\overline{\delta_o} \neq 0$ as long as the maximum post-buckling deflection $\overline{\delta_o}$ is small. The other possibility is that delamination will take place following buckling of the debonded region. This is the subject of the analysis contained in this paper.

There is one major assumption which lies at the root of the problem: the post-buckling configuration is taken to have a defined shape. This assumption has been adopted throughout researches on the problem (e. g. [2] and [3]). The present analysis takes the problem a step forward by assessing the effect of a resin rich layer on the post-buckling behavior and delamination.

THEORY

The applied load 'P' may be split between the outer and inner layers as shown in Figure (1). The attached portions of the top layer (Figure 2) may be regarded as two identical beams on elastic foundations, with a foundation, constant given by the resin modulus (E_r) divided by the resin film thickness (t_r) (corresponding to a simple Winker foundation stiffness). The differential equations governing the behaviour of the deflected shapes for the bulge and attached portions when loaded by the axial compressive force 'P' are represented respectively by [1];

$$\frac{d^4 w_1}{dx^4} + \left(\frac{P_1}{D}\right)\frac{d^2 w_1}{dx^2} = 0 \qquad \text{or}$$

$$\frac{d^4 w_1}{dx^4} + \alpha^2 \frac{d^2 w_1}{dx^2} = 0 \qquad \alpha^2 = \frac{P_1}{D} \tag{1}$$

$$\frac{d^4 w_2}{dx^4} + \alpha^2 \frac{d^2 w_2}{dx^2} + 4\beta^4 w_2 = 0 \tag{2}$$

where $\beta^4 = \frac{K}{4D}$, with $K = \frac{E_r}{t_r}$

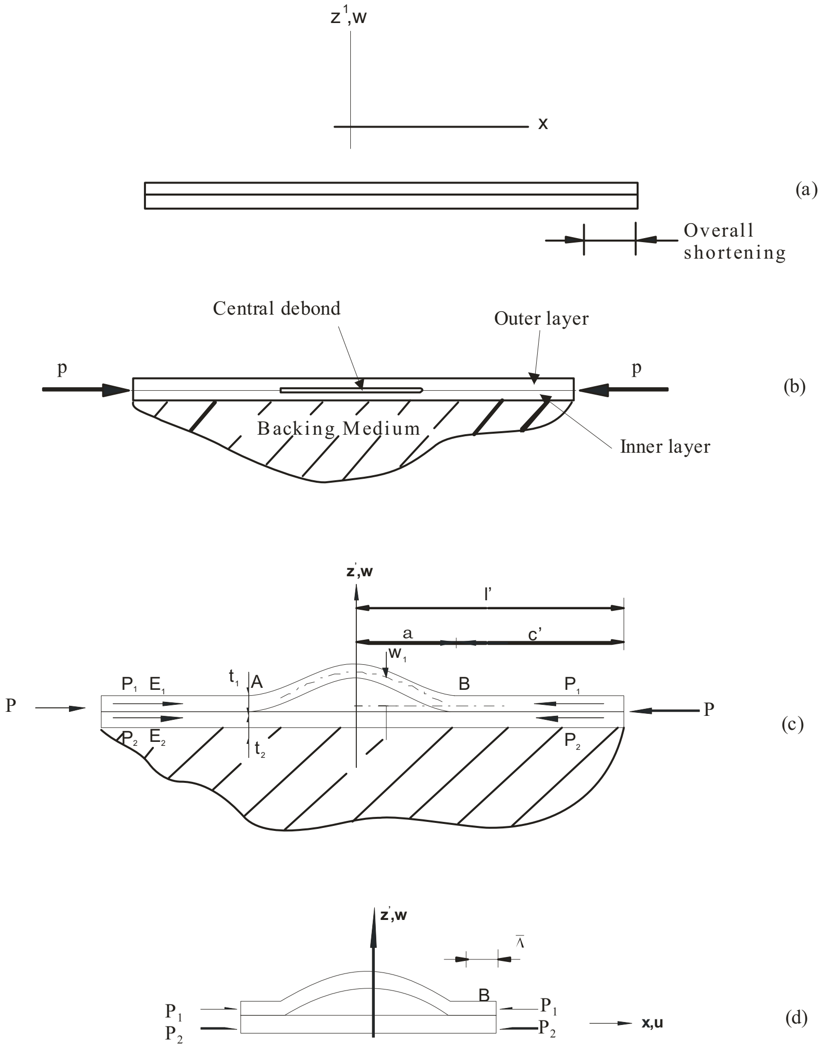

Figure 1: Buckling Delamination;
(a) Pre-loading Configuration,
(b) Pre-buckling Loaded Configuration,
(c) Buckled Debonded Layer,
(d) **Free body diagram for the delaminated portion**.

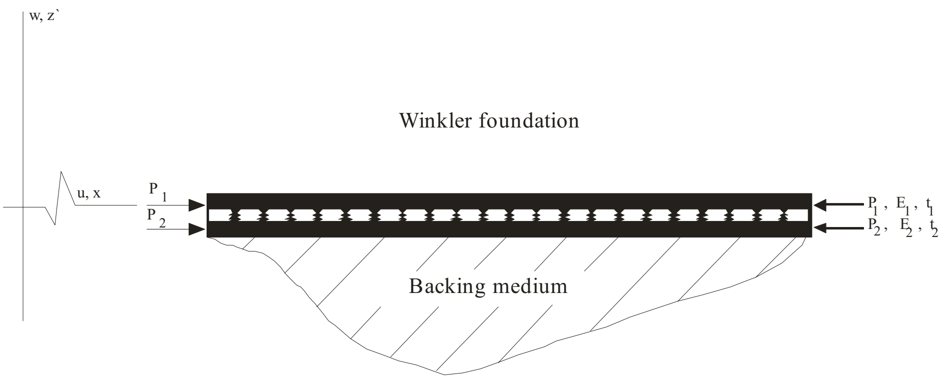

Figure 2: Attached region on winkler foundation.

Equations (1) and (2) have the following general solutions

$$w_1 = C_1 \cos\alpha x + \frac{C_2}{\alpha^2} \tag{3}$$

$$w_2 = e^{-\beta_1 x}\left[C_3 \cos(\beta_2 x) + C_4 \sin(\beta_2 x)\right] \tag{4}$$

where $\beta_1 = \sqrt{2\beta \sin(\phi/2)}$; $\beta_2 = \sqrt{2\beta \cos(\phi/2)}$

and $\phi = \arctan\sqrt{16\eta^4 - 1}$; $\eta = \beta/\alpha$

The constant C_1 to C_4 in Equations (3) and (4) may now be determined by imposing the continuity conditions of deflection, slope, bending moment and shear force along the delamination front between debonded and attached portions (point B in Figure (1c)). The continuity conditions yields;

$$C_1 \cos\mu + \frac{C_2}{\alpha^2} = Y_1\left(C_3 M_2 + C_4 M_1\right) \tag{5a}$$

$$-C_1 \alpha \sin\mu = Y_1\left[-C_3\left(\beta_1 M_2 + \beta_2 M_1\right) + C_4\left(-\beta_1 M_1 + \beta_2 M_2\right)\right] \tag{5b}$$

$$-C_1 \alpha^2 \cos\mu = Y_1\left[C_3\left(F_1 M_2 + F_2 M_1\right) + C_4\left(F_1 M_1 - F_2 M_2\right)\right] \tag{5c}$$

$$C_1 \alpha^3 \sin\mu = Y_1\left[C_3\left(h_1 M_2 - h_2 M_1\right) + C_4\left(h_2 M_2 + h_1 M_1\right)\right] \tag{5d}$$

where;
$F_1 = \beta_1^2 - \beta_2^2$, $F_2 = 2\beta_1\beta_2$, $M_1 = \sin\beta_2 a$, $M_2 = \cos\beta_2 a$, $h_1 = 3\beta_1\beta_2^2 - \beta_1^3$,
$h_2 = 3\beta_1^2\beta_2 - \beta_2^3$, $Y_1 = e^{-\lambda_1}$, $\lambda_1 = \beta_1 a$, $\mu = \alpha a$.

The last three of equations (5b, 5c, 5d) contain only C_1, C_3, and C_4 and may be solved simultaneously for these constants. The condition for a non-trivial solution is given by vanishing of the determinant of the coefficients for C_1, C_2 and C_4. Thus

$$\begin{vmatrix} -\alpha\sin\mu & \beta_1 M_2 + \beta_2 M_1 & \beta_1 M_1 - \beta_2 M_2 \\ -\alpha^2 \cos\mu & -F_1 M_2 - F_2 M_1 & -F_1 M_1 + F_2 M_2 \\ \alpha^3 \sin\mu & -h_1 M_2 + h_2 M_1 & -h_1 M_1 - h_2 M_2 \end{vmatrix} = 0 \tag{6}$$

Expanding the determinant and simplifying Equation (6) reduces to:

$$\tan\mu = \frac{2\chi_1 \mu \lambda'}{\mu^2 - 2\lambda'^2} \tag{7}$$

where $\lambda' = \beta a$ and $\chi_1 = \sqrt{2\sin(\phi/2)}$

Equation (7) may be solved graphically to yield the critical buckling load as shown in Figure (3) where both sides of the equations are plotted versus μ, noting that at buckling

$\alpha = \sqrt{P_E'/D}$, where P_E' is the critical buckling load for the delaminated layer. The load P_E' may differ from the Euler critical load P_E for a built-in strut because it incorporates the hinge effect offered by the elastic foundation. This effect, though small, manifests itself in smaller critical loads corresponding to lower values of E_r as shown in Figure (3).

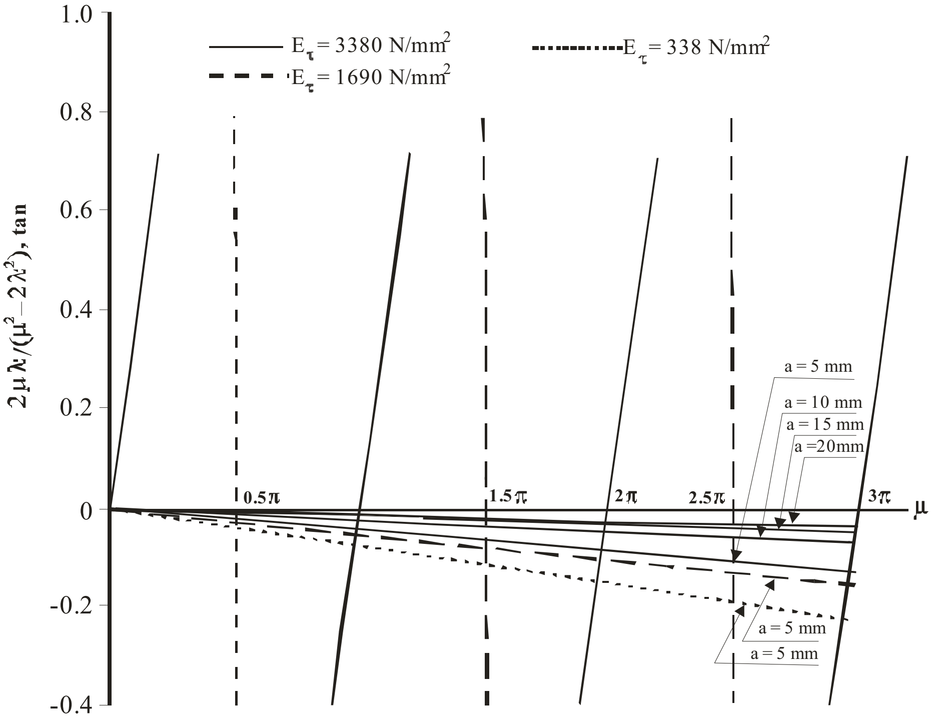

Figure 3: Graphical presentation of Equation (7).

Given that in general $P_E' < P_E$ for the problem under examination, it is permissible to write:

$$\alpha = \sqrt{(P_E'/D)} = \omega\pi/a \quad \text{or} \qquad P_E' = \frac{\omega^2\pi^2 D}{a^2}$$

as a solution to Equation (7), corresponding to the least buckling load; where ω is less than unity and, for a certain material, is dependent upon the debond half span length '*a*' as shown in Figure (3). The above dependence is clearly seen from Figure (4) where $\omega \to 1$ as $a \to \infty$. This is to say, for large values of 'a' the critical load P_E' approaches the Euler buckling load P_E. Another occasion when $P_E' \to P_E$ is that when the elastic foundation is infinitely stiff ($E_r \to \infty$). In fact, if E_r is very large $X_1 \to 1$ [see Equations (4) and (6)], also $\lambda' = \beta a \to \infty$ [see Equation (2)]; then Equation (7) becomes, tan μ = 0 which is possible if $\mu = a\sqrt{(P_E'/D)} = \pi$ or $P_E' = \pi^2 D/a^2 = P_E$, i.e. the Euler buckling load for a built-in strut.

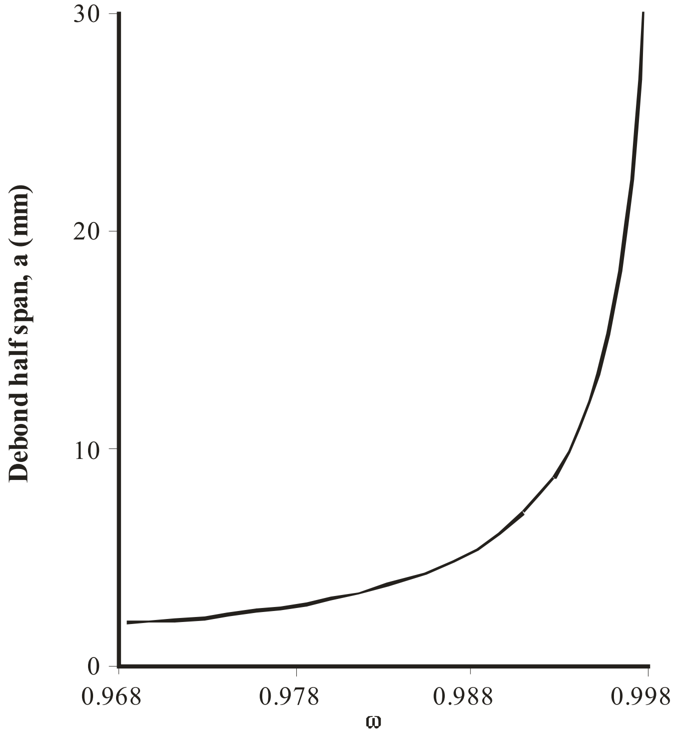

Figure 4: Reduction factor ω vs. debonded half span length.

POST-BUCKLING SHAPE

The constants C_2, C_3 and C_4 may be expressed in terms of the constant C_1 using Equation (5). Thus,

$$C_2 = \alpha^2 \cos\mu \left[\frac{1 + 4\eta^4 + 4\eta^2\left(\chi_1^2 - 1\right)}{2\eta^2\left(1 - 2\eta^2\right)} \right] C_1$$

$$C_3 = \frac{\cos\mu}{2Y_1\beta_2\beta^2} \left[\frac{\alpha^2\left(\beta_2 M_2 - \beta_1 M_1\right) + h_2 M_2 + h_1 M_1}{1 - 2\eta^2} \right] C_1 \tag{9}$$

$$C_4 = \frac{\cos\mu}{2Y_1\beta_2\beta^2} \left[\frac{\alpha^2\left(\beta_1 M_2 + \beta_2 M_1\right) + h_2 M_1 - h_1 M_2}{1 - 2\eta^2} \right] C_1$$

From Equations (9) and (3), remembering that at buckling $\alpha = \omega\pi/a$, we obtain

$$w_1 = \frac{\delta_o^*}{1 + Y(\lambda')} \cos(\rho x/a) + Y(\lambda') \tag{10}$$

where, $\delta_o^* = (w_1)_{x=0}$ is the debond mid-span maximum deflection, $\rho = \omega\pi$, and $Y(\lambda')$ is a function of λ' given by the following expression

$$Y(\lambda') = \frac{\rho^4 + 4\lambda'^4 + 4\lambda'^2\rho^2\left(\chi_1^2 - 1\right)}{2\lambda'\beta\left(\rho^2 - 2\lambda'\beta\right)} \cos\rho \tag{11}$$

It is seen from Equations (10) and (11) that for an infinitely stiff elastic foundation $\lambda' \to \infty$; $\omega \to 1$; $\cos\rho \to -1$, therefore

$w_1 \rightarrow \frac{\delta_o^*}{2}\left[1+\cos(\pi x/a)\right]=$ deflection for the built-in case.

The post-buckling maximum deflection shape given by Equation (10) will be completely defined once δ_o^* is known. Referring to Figure (1), the loading sequence which leads to buckling consists of assigning a uniform strain ε to the laminate which shortens as shown in Figure (1b), then the delaminated layer buckles Figure (1c), when the critical strain $\varepsilon'_E = \omega^2\pi^2 D/a^2 E_1 t_1$ is reached. If we assume that, in going from Figure (1b) to (1c), the length of the delaminated layer remains unchanged and its in-plane direct stress is the same as the buckling stress, (provided δ_o^* is relatively small) then the approach of the ends of the split as it buckles,

$$\overline{\Delta} = (2a)(\varepsilon - \varepsilon'_E) = \frac{1}{2}\int_{-a}^{a}\left(\frac{dw_1}{dx}\right)^2 dx \tag{12}$$

Equation (12), after substituting for w_1 from Equation (10) and integrating, gives:-

$$\delta_o^* = \frac{8a^2(\varepsilon - \varepsilon'_E)\left[1+Y(\lambda')\right]^2}{\rho(2\rho - \sin 2\rho)} \tag{13}$$

Substitution from Equation (13) into Equation (10) yields

$$w_1 = 2a\sqrt{\frac{2(\varepsilon - \varepsilon'_E)}{\rho(2\rho - \sin 2\rho)}}\left[\cos(\rho x/a) + Y(\lambda')\right] \tag{14}$$

ENERGY RELEASE RATE AND ELASTIC STRAIN ENERGY

The critical energy release rate g_c can be evaluated once the total strain energy per unit width in the laminate U is formulated. U may be split into four components U_b, U_{dc}, U_{at} and U_{in}; where U_b and U_{dc} are, respectively, the bending and direct compression energies for the delaminated layer, U_{at} is the strain energy of the attached portion and U_{in} is the strain energy of the inner layer (layer 2, as shown in Figure (1)). The strain energy component U_b may be evaluated using the equation:

$$U_b = 2\frac{D}{2}\int_0^a\left(\frac{d^2 w_1}{dx^2}\right)^2 dx \tag{15}$$

Therefore,

$$U_b = \frac{2aE_1 t_1\left(\varepsilon\varepsilon'_E - \varepsilon'^2_E\right)(2\rho + \sin 2\rho)}{2\rho - \sin 2\rho} \tag{16}$$

The other components of energy (U_{dc}, U_{at} and U_{in}) may be evaluated using the usual energy formula for direct stress and strain. Thus;

$$U_{dc} = \frac{aE_1 t_1 \varepsilon'^2_E}{1 - \nu_{\ell t}\nu_{t\ell}} \tag{17}$$

$$U_{at} = \frac{(\ell' - a)E_1 t_1 \varepsilon^2}{1 - \nu_{\ell t}\nu_{t\ell}} \tag{18}$$

$$U_{in} = \frac{\ell' E_2 t_2 \varepsilon^2}{1 - \nu_{\ell t}\nu_{t\ell}} \tag{19}$$

The total strain energy in the laminate U = $U_b + U_{dc} + U_{at} + U_{in}$; given by the components from Equations (16) through to (19). Can now be used in Equation (20) below (subject to imposing uniform overall applied strain ‘ε’ just sufficient to extend the already existing delamination with fixed grip conditions) to evaluate the strain energy release rate g, with the tacit assumption that the strain in the inner layer and the attached portion will remain unchanged after the debonded layer has buckled. Thus;

$$g = -\frac{dU}{da} \tag{20}$$

In a normalized form g becomes;

$$g_c = \frac{E_1 t_1^5 \pi^4 \omega^4}{144 a^4 \Gamma(1 - \nu_{\ell t}\nu_{t\ell})}\left\{3 + J^2 + 2Q(J-3) - \left(\frac{4a\omega^*}{\omega}\right)[1 + Q(J-2)] - 2aQ(J-1)\right\} \tag{21}$$

where,

$Q = [(1 - \nu_{\ell t}\nu_{t\ell})(2\rho + \sin 2\rho)]/(2\rho - \sin 2\rho)$; $J = \dfrac{\varepsilon}{\varepsilon'_E}$; $\omega^* = d\omega/da$ (plotted in Figure (5) versas “*a*” using Figure (3).

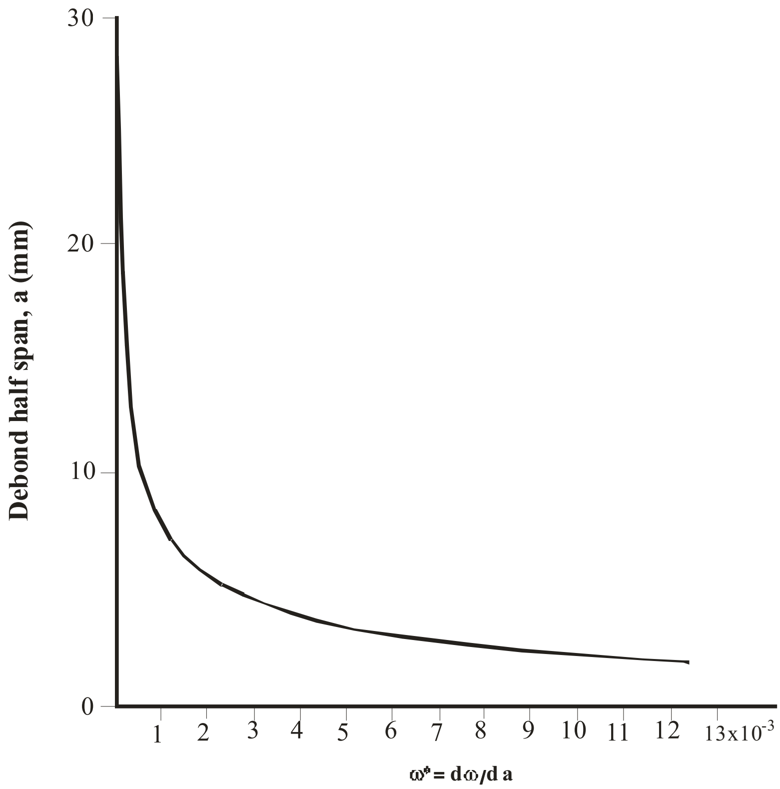

Figure 5: The rate of change of the factor ω with debond half span length a.

NUMERICAL RESULTS AND DISCUSSION

The following data, for unidirectional CFRP laminates [4,5] are used in this section study the delamination characteristics of an initially flat debonded layer:

$E_1 = 138500\,\mathrm{N/mm^2}$; $E_r = 3380\,\mathrm{N/mm^2}$; $\nu_{\ell t} = 0.3352$; $\nu_{t\ell} = 0.0223$

$t_1 = t_2 = 0.5\,\mathrm{mm}$; $t_r = 0.105\times10^{-4}\,\mathrm{mm}$; $\ell' = 75\,\mathrm{mm}$; $\Gamma = 0.26\,\mathrm{N/mm}$ [4].

Numerical computation of Equation (2) revealed that for J<1 (i.e $\varepsilon<\varepsilon_E'$) the normalized strain energy release rate was always negative, thus, no energy was released to propagate the existing split. Only after J≥1 (i.e. $\varepsilon \geq \varepsilon'_E$) does g_n become positive and therefore delamination is possible. The normalized strain energy release rate is plotted versus 'a' in Figure (6) for various values of J.

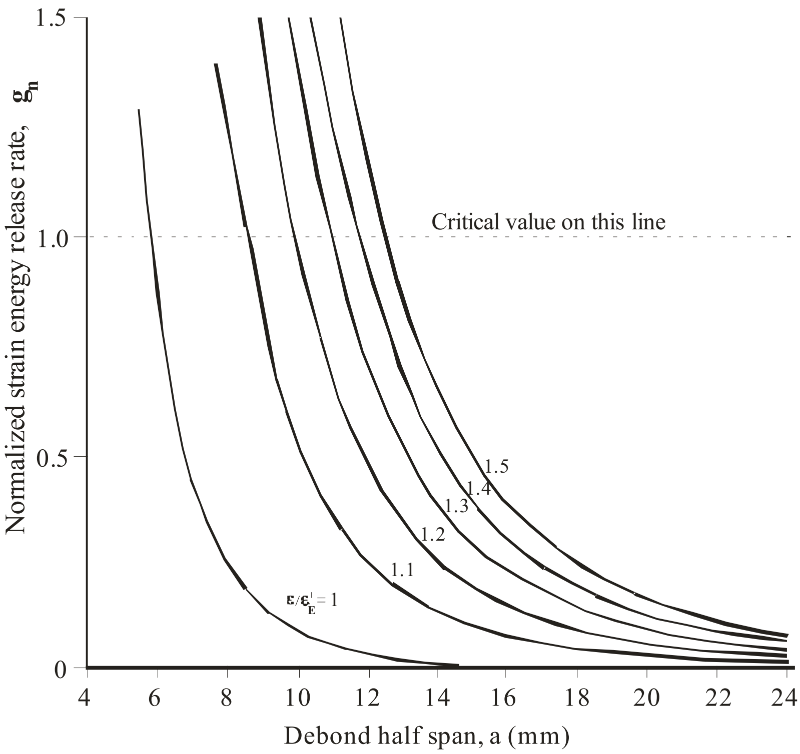

Figure 6: Normalized energy release rate vs. debond half span for various load ratios.

The g_n=1 horizontal dotted line represents the threshold for delamination growth. For points above this line splitting is always possible given that the energy release rate exceeds the toughness of separation Γ. It is also seen from Figure (6) that for an applied strain value $\varepsilon \leq 1.5\varepsilon'_E$ no delamination will occur for any $a \geq 12.75$ mm. The separation between possible and not-possible regions of delamination is shown in Figure (7) where the critical load ratio J is plotted versus the debond half span a.

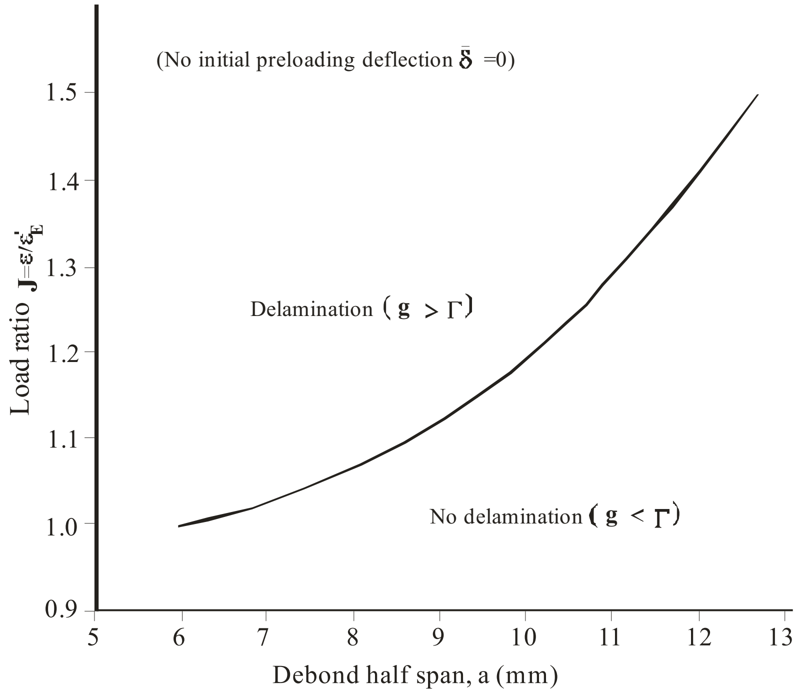

Figure 7: Critical load ratios vs. critical debonded half span.

CONCLUSIONS

A theoretical analysis based on beam-column theory and an energy release rate criterion, has been presented for the crack propagation of a layered fiber reinforced plastic strip in compression, in the presence of an initial flat debond. Account has been taken of a resin rich layer at the delaminating edge. The beam-column and beam on elastic foundation differential equations have been solved, respectively, for the shape of this post-buckled layer and the attached portion and the constants which appear in the solution have been determined through continuity conditions along the delamination front. The total strain energy has been evaluated for the partially debonded layer, and therefore the strain energy release rate. A typical set of design curves is given and discussed which shows the influence of the debonded length, applied strain and resin stiffness on loads required for splitting. It has been found here that delamination is not possible unless the delaminated layer buckles.

REFERENCES

[1] El-senussi, A. K., Webber, J. P. H., Blister Delamination Analysis in Fibre Reinforced Plastics using Beam-Column theory with an Energy Release Rate Criterion. Composite Structures, Vol.5, No.2, 1986, pp 125-142.

[2] Chai, H., Babcock, C. D., Knauss, W. G., One Dimensional Modeling of Fracture in Laminated Plates by Delamination Buckling. Int. J. Solids Structures, Vol.17, No.11, 1981, pp.1069-1083.

[3] Whitcom, J. D., Finite Element Analysis of Instability Related Delamination Growth. J. Comp. Materials, Vol.15, Sept. 1981, pp.403-426.

[4] El-Senussi, A. K., Webber, J. P. H., Critical Strain Energy Release Rate during Delamination of Carbon Fiber Reinforced Plastic Laminates, COMPOSITES, Vol.20, No.3, May 1989, pp.149-256.

[5] Ditcher, A. K., The non-Linear Stress-Strain Behavior of Carbon Fiber Reinforced Plastic and its Effect on the Analysis of Laminated Plates and Sandwich Beams. Ph. D. Thesis, March 1981, Aero. Eng. Dept., University of Bristol, U. K.

NOMENCLATURE

a	Debond half span
c'	Half attached length of outer layer
C_1, C_2, C_3, C_4	Constants of integration
D	Flexural rigidity of blister
E	Young's modulus
E_1, E_2, E_3	Young's moduli of outer, inner and resin, respectively
g	Energy release rate
g_n	Normalized strain energy release rate
J	Ratio of applied and buckling strains
k	Elastic foundation constant
ℓ'	Half span of outer layer
P	Applied load
P_1, P_2	Load/unit width in outer and inner layers, respectively.
P_E	Euler buckling load for delaminated layer
P'_E	Buckling load for delaminated
t	Total thickness of strip
t_1, t_2, t_3	Thickness of outer, inner and resin rich layers, respectively
u	Axial displacement
U	Strain energy/unit width
U_{at}	Strain energy/unit width for attached portion
U_b	Strain energy/unit width of bending
U_{dc}	Strain energy/unit width of direct compression
U_{in}	Strain energy/unit width for inner layer
w_1	Total deflection of blister layer
w_2	Deflection of attached portion (beam on elastic foundation)
x	Longitudinal variable coordinate
$Y(\lambda')$	Function of λ' defined by Eq.(11)
α	Square root of ratio between in-plane load and flexural rigidity
β	Defined below Eq.(2)
β_1, β_2	Defined below Eq.(4)
Γ	Surface energy tension
δ^*_o	Max. of post-buckled deflection of debonded layer
$\overline{\Delta}$	Shortening of blister
$\overline{\Delta}_o$	Shortening of undelaminated portion of outer layer
$\overline{\Delta}_1$	Total shortening of outer layer
ε	Applied longitudinal strain
ε'_E	Critical buckling strain for delaminated layer
η	Dimensionless ratio defined below Eq.(4)
λ'	Dimensionless term defined below Eq.(7)
λ_1	Dimensionless term defined below Eq.(5)
μ	Dimensionless term defined below Eq.(5)
$\nu_{\ell t}$	Poisson's ratio with respect to longitudinal fibre and transverse fibre directions (stress in fibre direction)
$\nu_{t\ell}$	Poisson's ratio with respect to transverse fibre and longitudinal fibre directions (stress in transverse direction)
π	Common constant (=3.141593)
ρ	Defined below Eq.(11)
ϕ	Defined below Eq.(4)
χ_1	Defined below Eq.(7)
ω	Reduction factor
ω^*	Defined below Eq.(21)